Supporting Information

The Destruction and Reorganization of Physically Cross-linked Network of Thermoplastic Polyurethane Depending on Its Glass Transition Temperature

Xuke Li [†*], *Hai Wang* [†], *Bijin Xiong* [†], *Elmar Pöselt* [‡], *Berend Eling* [‡], *Yongfeng Men* [†]

[†]State Key Laboratory of Polymer Physics and Chemistry, Changchun Institute of Applied Chemistry, Chinese Academy of Sciences, Renmin Street 5625, 130022 Changchun, P.R. China.

[‡]BASF -Polyurethanes GmbH, Elastogranstrasse 60, 49448 Lemförde, Germany.

*Corresponding Author: Xuke Li, Email: lixuker@gmail.com

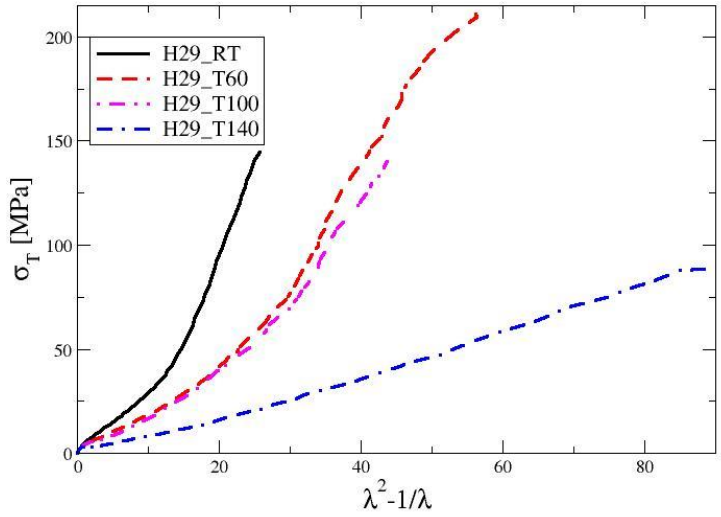

Figure S1. The stress-strain curve of TPU H29 deformed at different temperatures plotted in the form of σ_t vs. $\lambda^2 - \lambda^{-1}$.

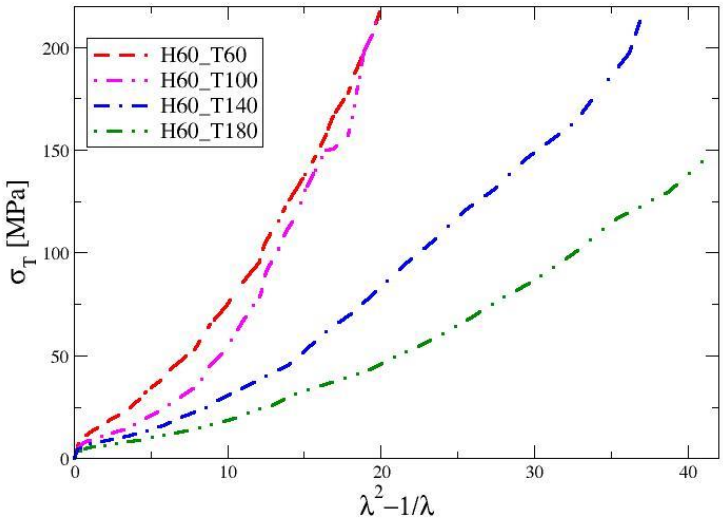

Figure S2. The stress-strain curve of TPU H60 deformed at different temperatures plotted in the form of σ_t vs. $\lambda^2 - \lambda^{-1}$.

Table S1. G_p, measured from the slope of the curve plotted in the form of σ_t vs. $\lambda^2 - \lambda^{-1}$, is shown as a function of the HSC and deformation temperature T. $G_p = \rho RT/\langle M_c \rangle$

Gp/[MPa]	H29	H42	H60
T25	2.56	4.36	--

T60	1.70	2.50	--
T100	1.47	1.70	2.07
T135	0.68	1.43	1.55
T170	--	0.89	1.14

Table S2. Average constraint molecular weight $\langle M_c \rangle$ are shown as a function of the HSC and deformation temperature *T*.

$\langle \boldsymbol{M_c} \rangle$ (g/mol)	H29	H42	H60
T25	1070	640	--
T60	1720	1230	--
T100	2120	1990	1610
T135	4830	2540	2240
T170	--	4340	3210

Table S3. Maximum elongation λ_{max} of TPUs with different HSCs deformed at different temperatures. The λ_{max} is the average values of five independent measurements.

	H29	H42	H60
T25	5.2	5.9	--
T60	8.1	6.4	--
T100	8.7	7.6	4.6
T135	8.2	7.8	6.1
T170	--	7.2	6.4

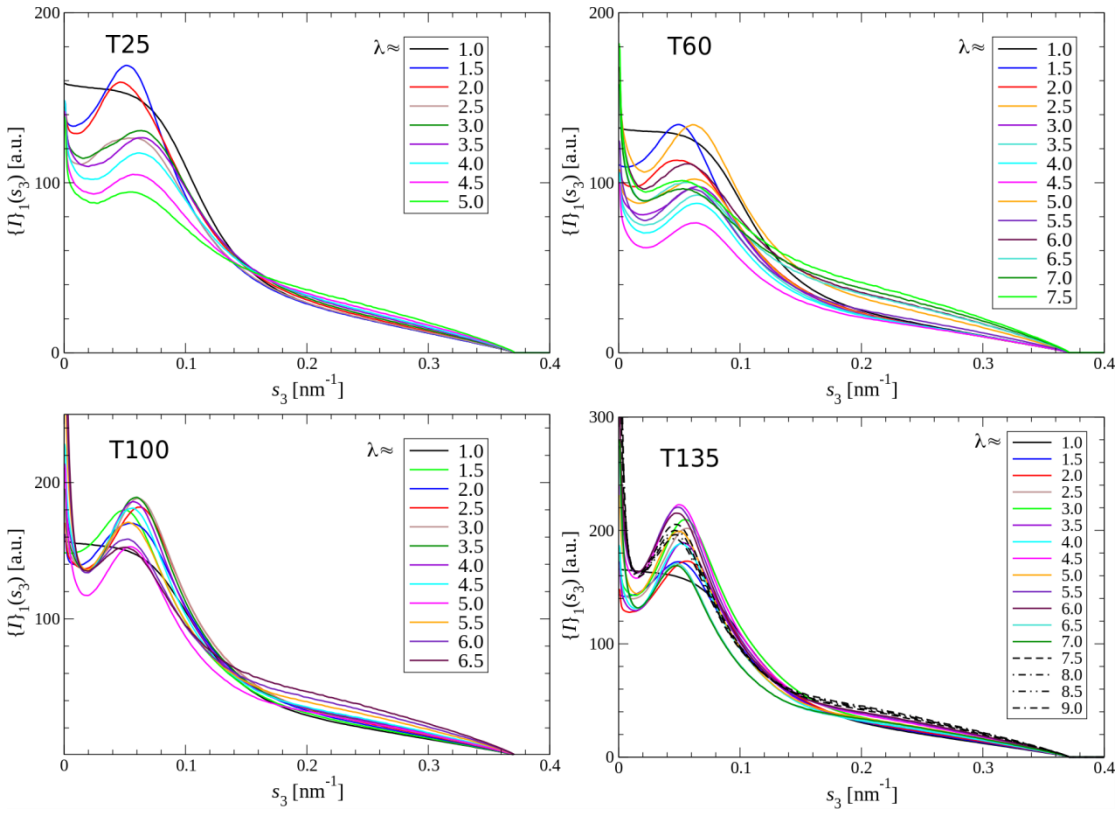

Figure S3: Vertical projection of SAXS pattern of sample H29 deformed at different temperatures varying as a function of elongation.

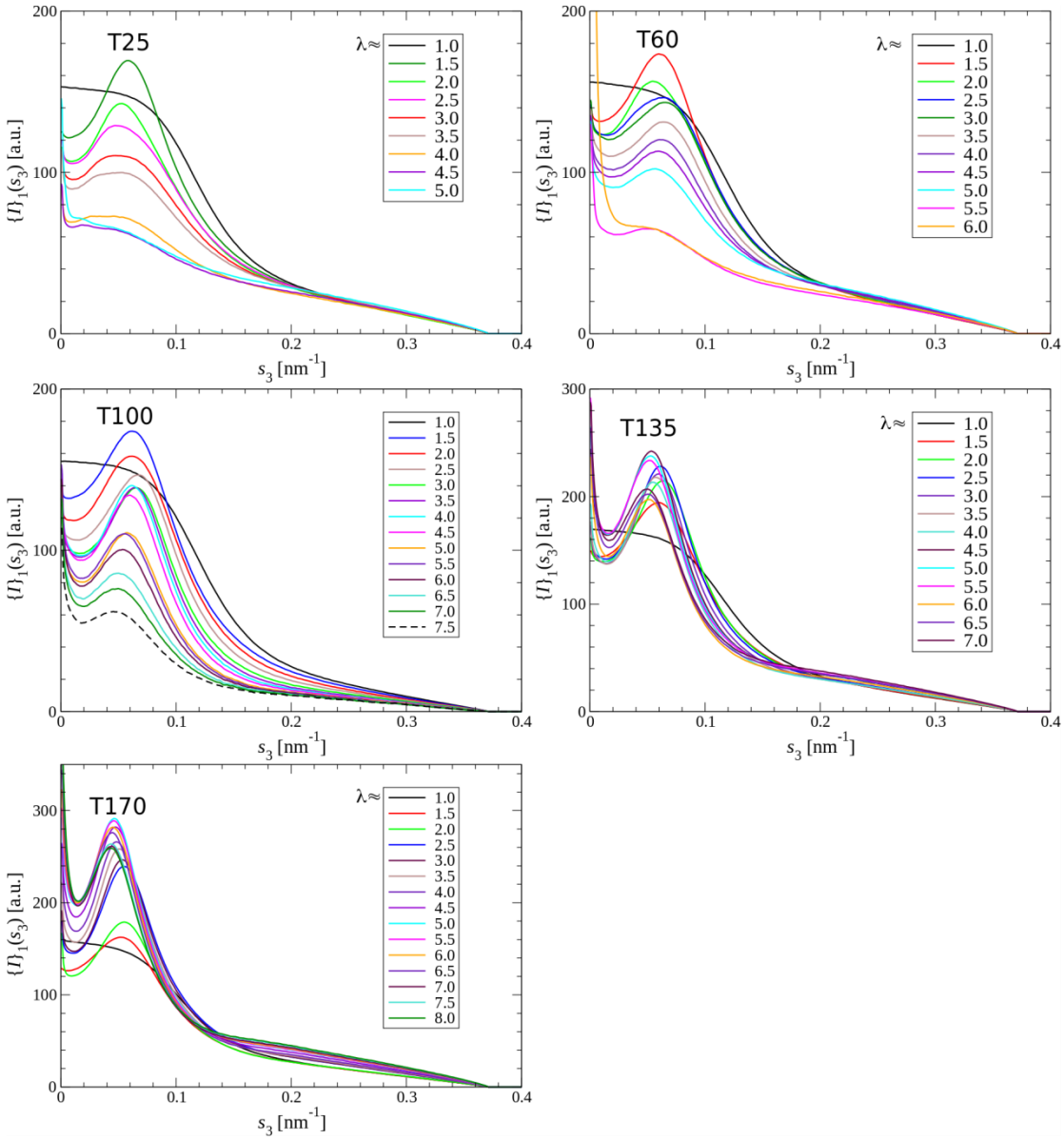

Figure S4: Vertical projection of SAXS pattern of sample H42 deformed at different temperatures varying as a function of elongation.

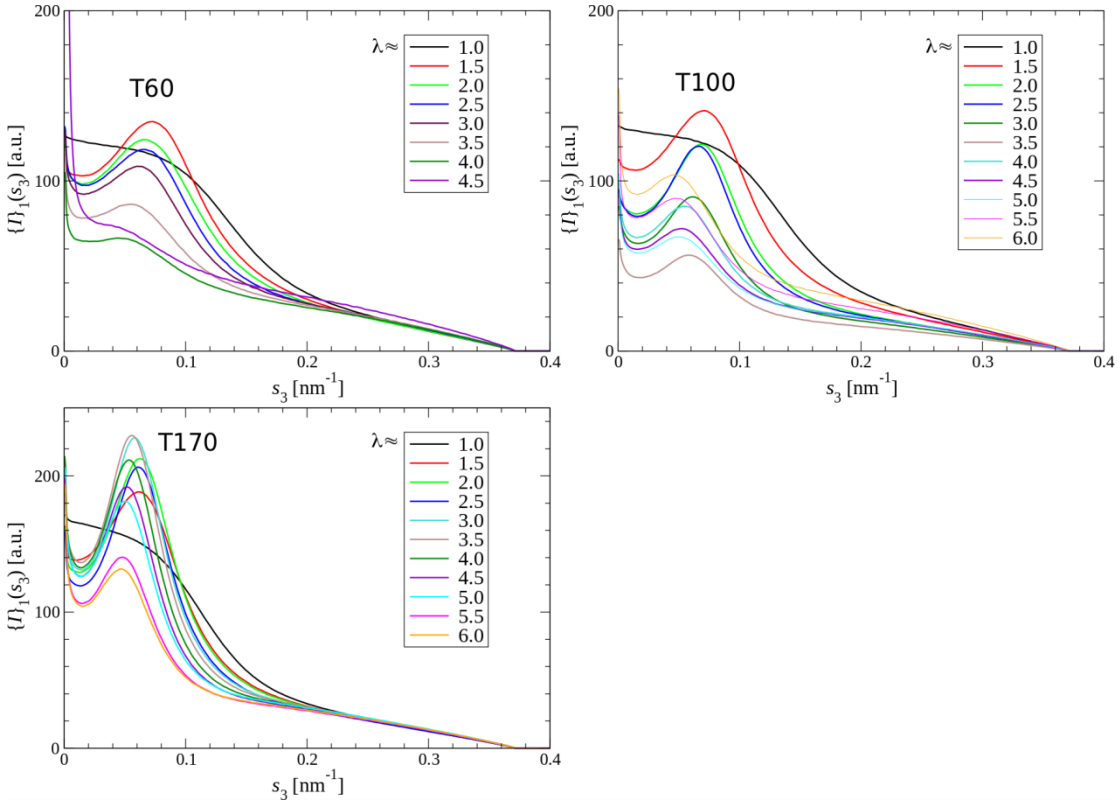

Figure S5: Vertical projection of SAXS pattern of sample H60 deformed at different temperatures varying as a function of elongation.

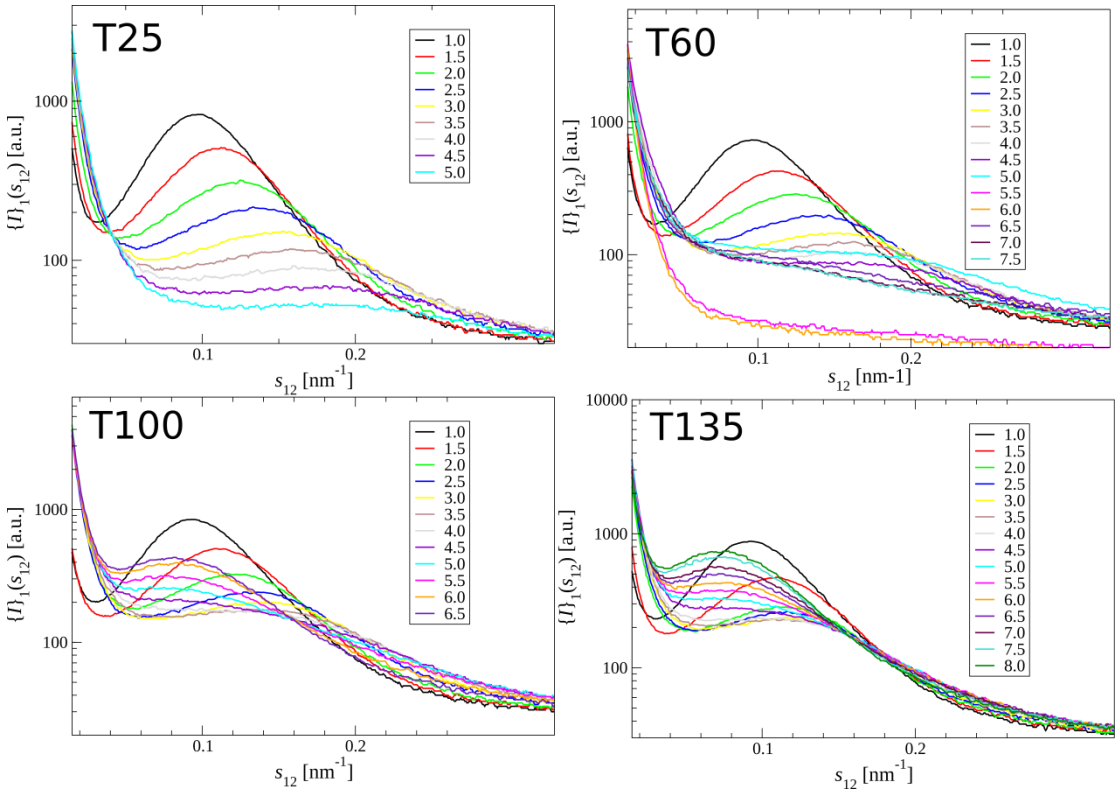

Figure S6: Horizontal projection of SAXS pattern of H29 deformed at different temperatures varying as a function of elongation.

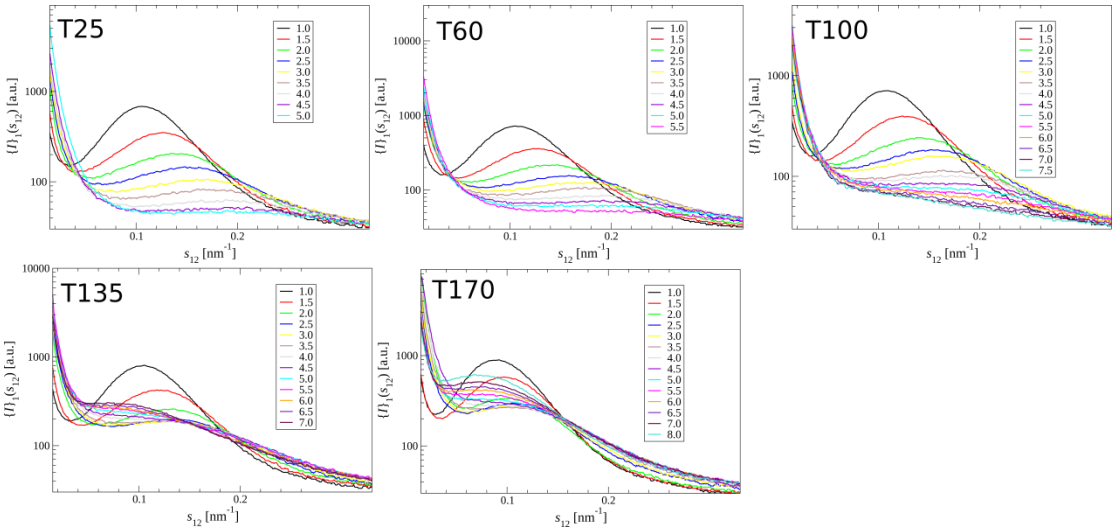

Figure S7: Horizontal projection of SAXS pattern of H42 deformed at different temperatures varying as a function of elongation.

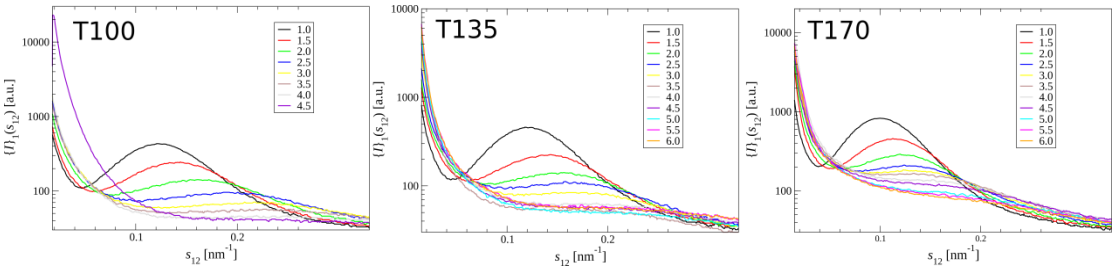

Figure S8: Horizontal projection of SAXS pattern of H60 deformed at different temperatures varying as a function of elongation.

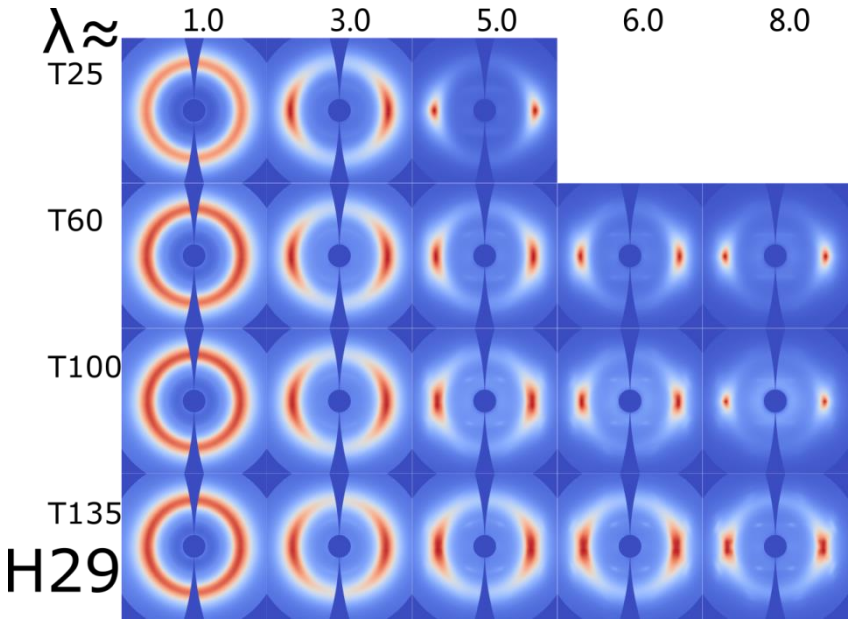

Figure S9: Selected WAXS patterns of H29 deformed at different temperatures. All WAXS patterns are projected onto the identical pseudo-color scale. The straining direction is vertical.

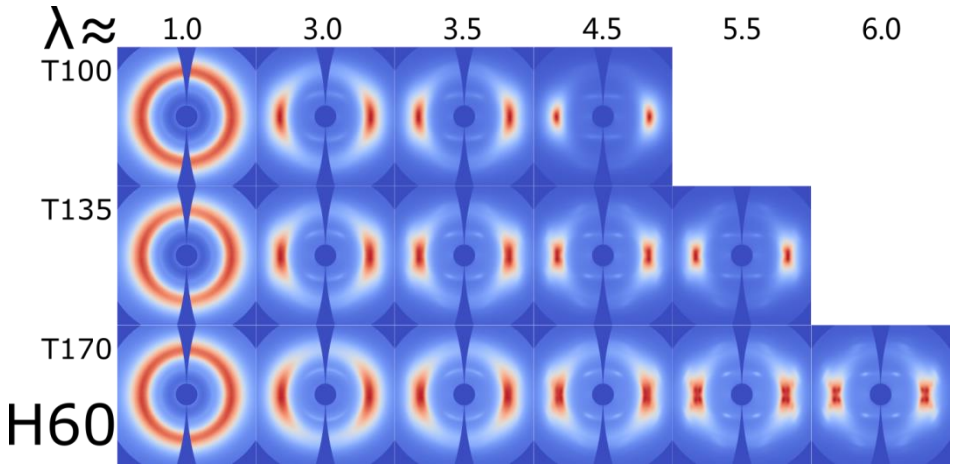

Figure S10: Selected WAXS patterns of H60 deformed at different temperatures. All WAXS patterns are projected onto the identical pseudo-color scale. The straining direction is vertical.

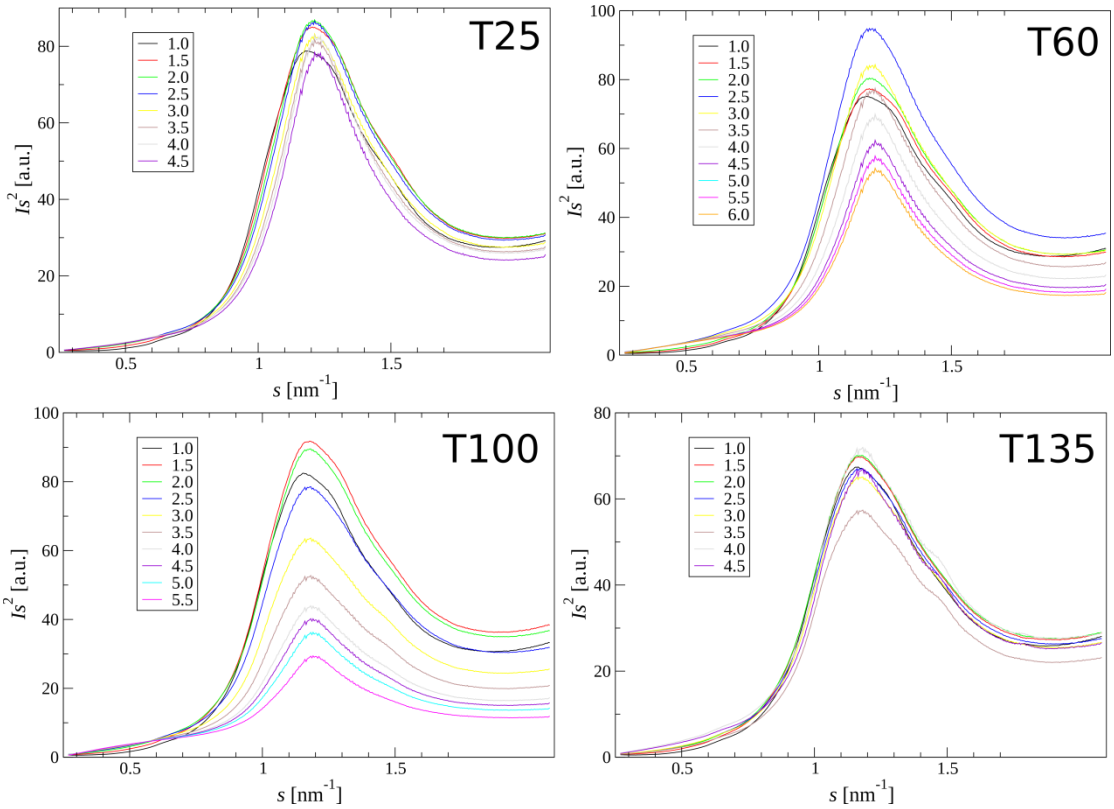

Figure S11: Spherical average[1,2] of WAXS pattern of H29 deformed at different temperatures as a function of elongation.

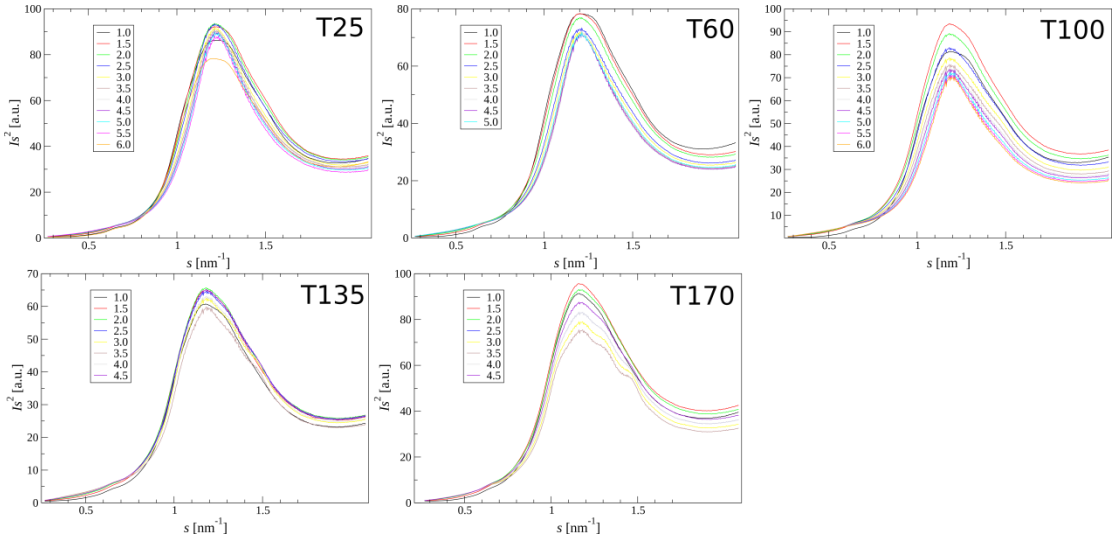

Figure S12: Spherical average of WAXS pattern of H42 deformed at different temperatures as a function of elongation.

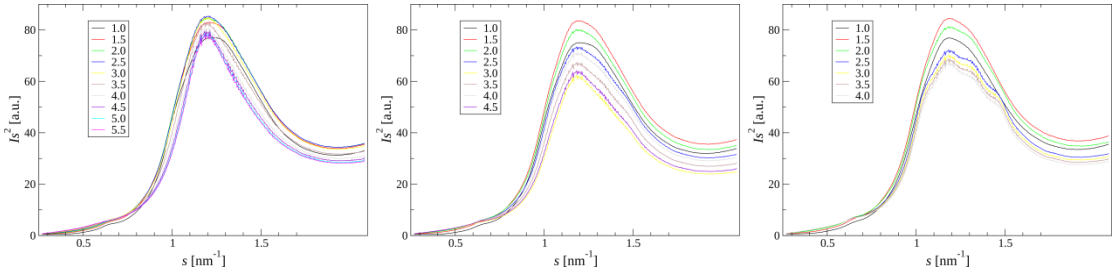

Figure S13: Spherical average of WAXS pattern of H60 deformed at different temperatures as a function of elongation.

Reference:

(1) Ruland, W. Fourier Transform Methods for Random-Layer Line Profiles. *Acta Crystallogr.* **1967**, *22* (5), 615–623.

(2) Stribeck, N. *X-Ray Scattering of Soft Matter*; Springer: Heidelberg, 2007. Page 130-131.